J. At. Mol. Sci.
doi: 10.4208/jams.021911.041411a

Vol. **2**, No. 4, pp. 368-376
November 2011

# First-principles study of electronic and magnetic properties and tetragonal distortion of the Heusler alloy $Mn_2NiAl$

Li-Jin Luo[a,*], Chong-Gui Zhong[a], Jing-Huai Fang[a], Peng-Xia Zhou[a], Yong-Lin Zhao[a], and Xue-Fan Jiang[b]

[a] *School of Science, Nantong University, Nantong 226007, China*
[b] *Jiangsu Key Laboratory of Advanced Functional Materials, Changshu Institute of Technology, Changshu 215500, China*

Received 19 February 2011; Accepted (in revised version) 14 April 2011
Published Online 28 June 2011

**Abstract.** The crystal structure, tetragonal distortion, magnetism, electronic structure and pressure response of $Mn_2NiAl$ are calculated by first-principles method based on the density functional theory. The calculations show, the equilibrium structure of $Mn_2NiAl$ in the cubic austenitic phase is the MnMnNiAl structure with Mn atoms occupy A and B sites and two Mn atoms occupy inequivalent positions. In the process of transform from a cubic to a tetragonal structure, $Mn_2NiAl$ alloys exhibit a stable martensitic phase near $c/a = 1.24$. In both the austenite and martensite phases, Mn atoms are the main contributors to the magnetism in $Mn_2NiAl$, $Mn_2NiAl$ alloys show ferrimagnetism due to antiparallel but unbalanced magnetic moments of Mn(A) atom and Mn(B) atom. The direct d-d exchange interactions between Mn(A) atom and Mn(B) atom are weak because of small overlap of d-projected DOS of Mn(A) atom and Mn(B) atom nearby the Fermi level, but the intra-atomic interactions in Mn atoms are strong, this is the reason why the $Mn_2NiAl$ alloys show ferrimagnetism. The findings strongly suggests that $Mn_2NiAl$ alloys would behave like a magnetic shape memory alloy.

**PACS**: 75.50.Cc, 71.15.Nc, 81.30.Kf

**Key words**: first-principles, tetragonal distortion, martensite phase transformation, ferrimagnetism

## 1 Introduction

Magnetic shape memory alloy (MSMA) is a newly-developed shape memory material. It has not only thermoelastic shape memory effect as traditional shape memory alloy does by temperature control but also magnetic shape memory effect (MSME) by magnetic field control.

*Corresponding author. *Email address:* luolijin1964@126.com (L. J. Luo)

 

Compared with other intelligent driving materials like traditional shape memory alloy, piezoceramics, magnetostriction material, etc., MSMA has greater reinstate strain, output of stress and higher response frequency, making up the slowness of traditional shape memory alloy in response frequency and the shortage of piezoceramics and magnetostriction material in reinstate strain, and it is considered an ideal driving and sensing material, with a prospect of wide application.

Of the researches on MSMA, Heusler alloy is one of the materials which are conducted the most [1–3]. The findings have shown that a certain amount of Heusler alloys have MSME. The earliest finding, with regard to Heusler alloy with MSME that draws attention and stimulates deep research, is $Ni_2MnGa$ [4–6]. Afterwards, Ni-Fe-Ga [7, 8], Co-Ni-Ga(Al) [9, 10], Ni-Mn-In(Sn, Sb) [11], etc., have been successively found with MSME.

Recent researches in theory and experiments have indicated that $Mn_2NiGa$, a new Heusler alloy, also has MSME [12], which exhibits a martensitic transformation around room temperature and an excellent two-way shape memory behavior with a strain of 1.7% in single crystal samples. It was also found that $Mn_2NiGa$ has a Curie temperature up 588 K being much higher than that of studied $Ni_2MnGa$, whose Curie temperature is about 370 K. However, its ordered structure is different from the ordered structure of tradition $L2_1$ structure, i.e. Mn atoms occupy A and B sites, Ni atom C site and Ga atom D site, with a space group of $F\overline{4}3m$.

In this work, we mainly research another Heusler alloy $Mn_2NiAl$. Because it, like $Mn_2NiGa$, belongs to MnNi Heusler alloy, and Al and Ga belong to *sp* element as well, $Mn_2NiAl$ may be considered a potential candidate for magnetic shape memory material. We investigate the crystal structure, tetragonal distortion, magnetism, electronic structure and pressure response of the $Mn_2NiAl$ by first-principles method based on the density functional theory. The results show that $Mn_2NiAl$ alloys exhibit a stable martensitic phase near $c/a = 1.24$ in the process of transform from a cubic to a tetragonal structure, and $Mn_2NiAl$ alloys show ferrimagnetism in both austenite and martensite phases. These discoveries found strong evidence that $Mn_2NiAl$ alloys would behave like a magnetic shape memory alloy.

## 2 Calculation method

The calculations are performed with the projected augmented wave (PAW) method based on the density functional theory, where the exchange-correlation potential is treated with the generalized gradient approximation of Perdew and Wang (PW91-GGA), the projected augmented wave (PAW) method is used in the interaction between ion and electron. The wavefunctions are expressed as a supposition of plane waves with a cut-off energy 400 eV. We choose k-points according to the scheme proposed by Monkhorst and Pack. A k-mesh parameters $19\times19\times19$ is adopted in the calculations of relaxation and static state, and $23\times23\times23$ is used in the calculations of DOS. The convergence criterion for total energy is $10^{-4}$ eV/au$^3$. The specific calculations are carried out with a package called VASP(Vienna abinitio simulation package) [13].

In the calculation, the structure of $Mn_2NiAl$ in the cubic austenitic phase is taken to be

that of the cubic $L2_1$ consisting of four interpenetrating fcc sublattices at $(0,0,0)$ A position, $(1/4,1/4,1/4)$ B position, $(1/2,1/2,1/2)$ C position and $(3/4,3/4,3/4)$ D position. Based on the different alignments of Mn, Ni, and Al atoms in four fcc sublattices, two ordered structures can be obtained. One is Mn atoms occupy A and C sites, Ni atom B site, Al atom D site and these two Mn atoms occupy equivalent positions (called it MnNiMnAl structure, see Fig. 1(a)). The other is Mn atoms occupy A and B sites, Ni atom C site, Al atom D site and these two Mn atoms occupy non-equivalent positions (called it MnMnNiAl structure, see Fig. 1(b)).

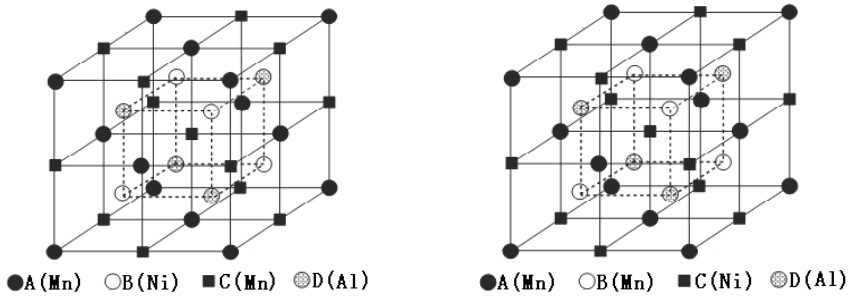


(a) (b)

Figure 1: The structure of $Mn_2NiAl$ where (a) Mn atoms occupy equivalent positions (MnNiMnAl structure) and (b) Mn atoms occupy non-equivalent positions (MnMnNiAl structure).

## 3 Results and discussion

### 3.1 The optimization of the cubic austenitic structure

In order to obtain the optimized structure of $Mn_2NiAl$ in the cubic phase, the total energies ($E_{tot}$) in the cubic phase are calculated to determine the minimum energy atom position (MnNiMnAl or MnMnNiAl) and the magnetic state (paramagnetic or ferromagnetic), i.e., calculating the $E_{tot}$ as a function of the unit cell volume for MnNiMnAl and MnMnNiAl structure in the cubic phase for different magnetic states (see Fig. 2). In these four situations (i.e., para MnNiMnAl, para MnMnNiAl, ferro MnNiMnAl and ferro MnMnNiAl), $E_{tot}$ as a function of cell volume exhibit a parabolic behaviour and the minimum determines the optimized lattice constant. It shows that the energies of the ferromagnetic states are lower compared to the paramagnetic states for both MnNiMnAl and MnMnNiAl structure over the studied unit cell volume range, and in both ferromagnetic states, the energy of the MnMnNiAl ferromagnetic state is lowest. Thus, it can be concluded that the equilibrium structure of $Mn_2NiAl$ in the cubic austenitic phase is the MnMnNiAl structure with the ferromagnetic state. The equilibrium volume in the cubic austenitic phase is 194.0643 $Å^3$ (shown by the arrow), and the corresponding lattice constant is $a = 5.7896$ Å.

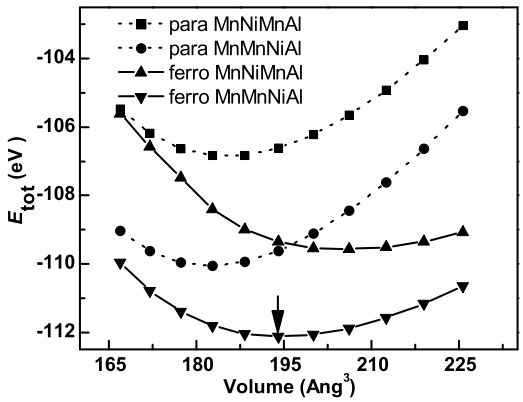


Figure 2: Total energy ($E_{\text{tot}}$) as a function of unit cell volume for MnNiMnAl and MnMnNiAl structure in the cubic phase for different magnetic states.

## 3.2 Tetragonal distortion and acquiring a stable martensitic phase

The martensitic transition involves a structural transition from cubic to a lower symmetry phase with decreasing temperature. In order to determine whether there is a stable martensitic phase, we have calculated $E_{\text{tot}}$ as a function of the distortion in the lowest energy magnetic state. It consists of two steps: in the first step $E_{\text{tot}}$ has been calculated as a function of the tetragonal $c/a$ ratio in the process of tetragonal distortion with fixed volume (volume held fixed at that of the cubic austenitic phase), the calculation result shows in Fig. 3(a). There is a

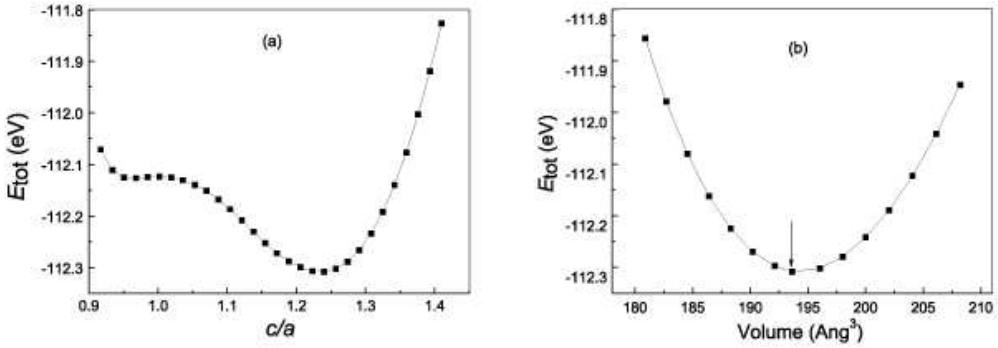


Figure 3: (a) The calculated total energies ($E_{\text{tot}}$) of $Mn_2NiAl$ as a function of the tetragonal $c/a$ ratio in the process of tetragonal distortion with fixed volume. (b) The calculated total energies ($E_{\text{tot}}$) of $Mn_2NiAl$ as a function of the unit cell volume of the tetragonal martensitic phase.

low-energy local minimum near $c/a=1.24$ with total energy lower than the cubic austenitic phase, it indicates that $Mn_2NiAl$ alloys exhibit a stable martensitic phase near $c/a=1.24$. In the next step, to reach global $E_{tot}$ minimum in the tetragonal martensitic phase, the unit cell volume is varied keeping $c/a$ fixed at 1.24, the calculation result shows in Fig. 3(b). The $E_{tot}$ minimum is obtained at the unit-cell volume of 193.6329 Å$^3$ (shown by the arrow). Thus, the equilibrium lattice constants in the tetragonal martensitic phase are $a=5.3892$ Å and $c=6.6670$ Å. On the other hand, although there is a large change in crystal structure, there is almost novolume change between the austenitic and the martensitic phases. The structural phase transition is nearly volume conserving, which is a characteristic of a shape memory alloy [14].

### 3.3 Magnetism

In order to investigate the magnetism of $Mn_2NiAl$ (MnMnNiAl structure) in austenite and martensite phases respectively, we optimize their lattice parameters by calculating the total energy as a function of the lattice parameters (as mentioned above), and calculate their total magnetic moments and spin magnetic moments for each atom at equilibrium lattice constants. The results of calculation are given in Table 1. It can be seen from Table 1 that: a) In both austenite and martensite phases, Mn atoms are the main contributors to the total moments in $Mn_2NiAl$, but the contributions of Ni and Al atoms to the total moments are potty. b) In both austenite and martensite phases, $Mn_2NiAl$ alloys show ferrimagnetism due to antiparallel but unbalanced magnetic moments of Mn(A) and Mn(B) atoms.

It is believed that the magnetism, especially in 3d alloys, is predominantly determined by the immediate environment around potentially magnetic atoms. The magnetism of Mn(A) and Mn(B) atoms are different because of different local surrounding, a Mn(A) atom is surrounded by four Al and four Mn(B) atoms, and a Mn(B) atom is surrounded by four Ni and four Mn(A) atoms.

Table 1: The total magnetic moments and spin magnetic moments for each atom of $Mn_2NiAl$ in austenite and martensite phases respectively.

| Parameter | Austenite | Martensite |
|---|---|---|
| Total magnetic moment/ $\mu_B$ | 1.244 | 1.087 |
| Spin magnetic moment(Mn(A)) / $\mu_B$ | -1.941 | -1.988 |
| Spin magnetic moment(Mn(B)) / $\mu_B$ | 2.866 | 2.766 |
| Spin magnetic moment(Ni) / $\mu_B$ | 0.298 | 0.288 |
| Spin magnetic moment(Al) / $\mu_B$ | 0.002 | 0 |

### 3.4 Density of state (DOS)

The density of states (DOS) of material explains clearly its magnetic state and the electronic structure. The calculated total DOS, Mn(A)-*d*-projected DOS, Mn(B)-*d*-projected DOS, Ni-d-

projected DOS, Al-$s$-projected DOS and Al-p-projected DOS of $Mn_2NiAl$ (MnMnNiAl structure) in austenite and martensite phases are presented in Figs. 4 and 5 respectively. It can be seen from these figures, the distribution of Mn(A)-$d$-projected DOS and Mn(B)-$d$-projected DOS are obviously different in both austenite and martensite phases. For Mn(A)-$d$-projected DOS, the spin-up states are mostly situated above the Fermi level, and the spin-down states are mostly situated below the Fermi level. While for Mn(B)-$d$-projected DOS, the spin-up states are mostly situated below the Fermi level, and the spin-down states are mostly situated above the Fermi level. Therefore there is a small overlap between Mn(A)-$d$-projected DOS and Mn(B)-$d$-projected DOS nearby the Fermi level, and there is large splitting in DOS between spin-up and spin-down states in both phases, as well as leads to greater magnetic moments (the magnetic moments of Mn(A) atoms are -1.941$\mu_B$ (austenite) and -1.988$\mu_B$ (martensite), Mn(B) atoms are 2.866$\mu_B$ (austenite) and 2.766$\mu_B$ (martensite)).

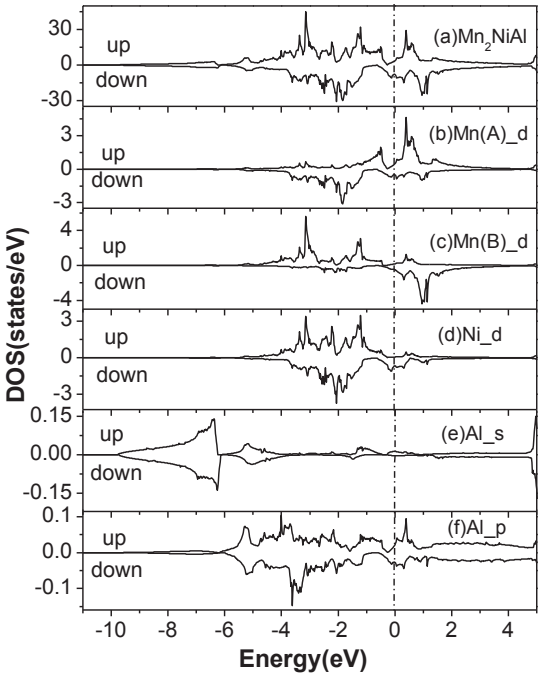


Figure 4: The calculated total and atom-projected DOS for $Mn_2NiAl$ (MnMnNiAl structure) in austenite: (a) the total DOS; (b) Mn(A)-$d$-projected; (c) Mn(B)-$d$-projected; (d) Ni-$d$-projected; (e) Al-$s$-projected; (f) Al-$p$-projected.

Comparing the austenite DOS with the martensite DOS, we discover that the DOS of these two states are similar on the whole, i.e., the $Mn_2NiAl$ total DOS nearby the Fermi level is mainly determined by Mn(A)-$d$-projected DOS and Mn(B)-$d$-projected DOS, and there is a small overlap between Mn(A)-$d$-projected DOS and Mn(B)-$d$-projected DOS nearby the Fermi level. It shows that the direct $d$-$d$ exchange interactions between Mn(A) and Mn(B) atoms

are weak, but the intra-atomic interactions in Mn atoms are strong, which lead to the large spin-splitting in DOS between spin-up and spin-down states, resulting in large localized spin magnetic moments in Mn atoms. Here the antiparallel alignment between Mn(A) and Mn(B) atoms is maintained by a weak interaction of the direct *d*-*d* exchange, but the ferromagnetic coupling within each sublattice is maintained by the superexchange interaction via *sp* electrons in Al atom. This is the reason why the $Mn_2NiAl$ alloys show ferrimagnetism in both austenite and martensite phases.

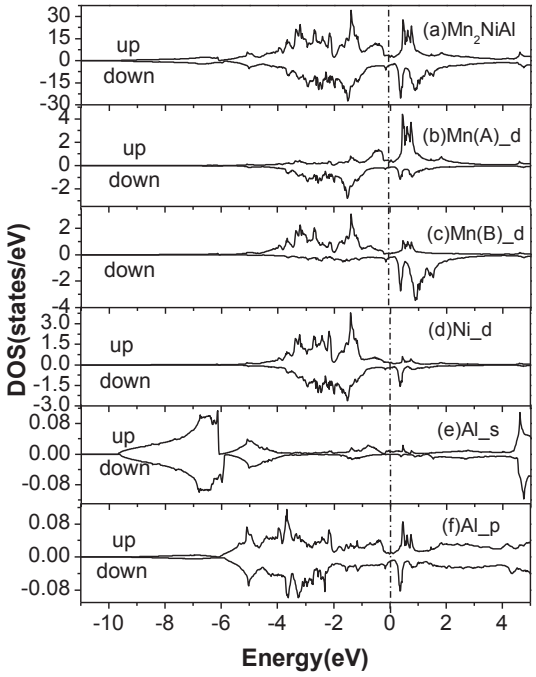


Figure 5: The *P*-*V* relation for $Mn_2NiAl$.

## 3.5 Pressure response

The bulk modulus $B$ expresses the material resistance to hydrostatic pressure, in general it is defined by

$$B = -\frac{\partial P}{\partial V} = V\frac{\partial^2 E}{\partial V^2}, \tag{1}$$

where $E$ is the total ground-state energy, $P$ is the pressure and $V$ is volume. $B_0$ and $B'$ are the bulk modulus and its pressure derivative at zero pressure, they are obtained from a fit of the

Murnaghan EOS to the energy as a function of volume. The Murnaghan EOS is given by

$$E(V)=\frac{B_0V}{B'(B'-1)}\left[\left(\frac{V_0}{V}\right)^{B'}+B'\left(1-\frac{V_0}{V}\right)-1\right]+E_0, \tag{2}$$

where $V_0$ and $E_0$ represent the volume and the total ground-state energy at zero pressure, respectively. Thus, our results of calculation for $Mn_2NiAl$ are $B_0=125.69$ GPa and $B'=5.47$. In comparison with related compounds the obtained value of $B_0$ for $Mn_2NiAl$ is less than that for $Ni_2MnGe$ (138.97 GPa) [15] or $Ni_2MnGa$ (170 GPa) [16] or $Ni_2MnB$ (247.7 GPa) [17], we expect that $Mn_2NiAl$ is the more compressible material than that mentioned above $Ni_2MnGe$ and $Ni_2MnGa$ and $Ni_2MnB$ compounds.

The pressure-volume relation can be obtained using the Murnaghan EOS as the negative volume derivative of the total energy. The pressure can be expressed as

$$P(V)=\frac{B_0}{B'}\left[\left(\frac{V_0}{V}\right)^{B'}-1\right]. \tag{3}$$

According to the calculated $B_0$ and $B'$, we can draw the pressure-volume relation of $Mn_2NiAl$ using Eq. (3) (Fig. 6). From Fig. 6, we would expect that a pressure about 13.28 GPa is needed to compress $Mn_2NiAl$ sample to about 8% of its original volume.

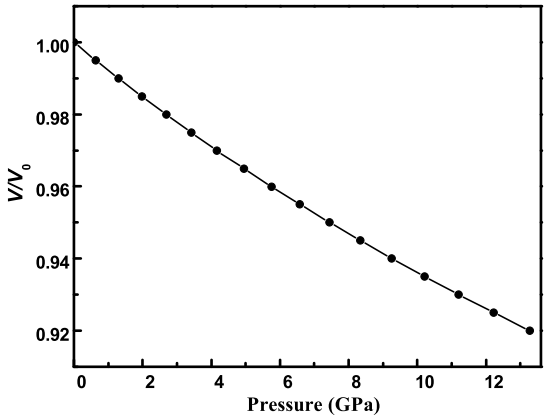


Figure 6: The $P$-$V$ relation for $Mn_2NiAl$.

## 4 Conclusions

The equilibrium structure of $Mn_2NiAl$ in the cubic austenitic phase is the MnMnNiAl structure with A, B, C and D sites occupied by Mn, Mn, Ni and Al atoms, respectively. In the

process of transform from a cubic to a tetragonal structure, there is a low-energy local minimum near $c/a=1.24$, it indicates that $Mn_2NiAl$ alloys exhibit a stable martensitic phase near $c/a=1.24$. In both austenite and martensite phases, Mn atoms are the main contributors to the magnetism in $Mn_2NiAl$, $Mn_2NiAl$ alloys show ferrimagnetism due to antiparallel but unbalanced magnetic moments of Mn(A) and Mn(B) atoms. The direct $d$-$d$ exchange interactions between Mn(A) and Mn(B) atoms are weak because of small overlap of $d$-projected DOS of Mn(A) and Mn(B) atoms nearby the Fermi level, but the intra-atomic interactions in Mn atoms are strong, this is the cause of the $Mn_2NiAl$ alloys show ferrimagnetism. This is strong evidence that $Mn_2NiAl$ alloys would behave like a magnetic shape memory alloy.

**Acknowledgments.** This work was supported by the National Natural Science Foundation of China under Grant Nos. 10974104, 30970754, and 10874021, the Natural Science Foundation of Jiangsu Province of China under Grant No. BK2006047, the Natural Science Foundation of the Jiangsu Higher Education Institutions of China under Grant No. 06KJA43014.

**References**

[1] G. D. Liu, J. L. Chen, Z. H. Liu, *et al.*, Appl. Phys. Lett. 87 (2005) 262504.
[2] H. Z. Luo, F. B. Meng, Z. Q. Feng, *et al.*, J. Appl. Phys. 107 (2010) 013905.
[3] W. J. Xie, X. F. Tang, and Q. J. Zhang, Chinese Phys. B 16 (2007) 3549.
[4] J. F. Wan and J. N. Wang, Physica B 355 (2005) 172.
[5] G. L. Xu, J. Z. Ma, J. D. Chen, *et al.*, Chinese Phys. B 18 (2009) 744.
[6] G. Jakob and H. J. Elmers, J. Magn. Magn. Mater. 310 (2007) 2779.
[7] H. X. Zheng, J. Liu, M. X. Xia, and J. G. Li, J. Alloys Compd. 387 (2005) 265.
[8] S. Aich, S. Das, I. A. Al-Omari, *et al.*, J. Appl. Phys. 105 (2009) 07A943.
[9] S. Tetsuji, K. Yukihiko, and K. Toshiro, J. Appl. Phys. 103 (2008) 07B322.
[10] F. B. Meng, H. J. Guo, G. D. Liu, *et al.*, Chinese Phys. B 18 (2009) 3031.
[11] X. Moya, L. Mañosa, A. Planes, *et al.*, Mater. Sci. Eng. A 438-440 (2006) 911.
[12] G. D. Liu, X. F. Dai, S. Y. Yu, *et al.*, Phys. Rev. B 74 (2006) 054435.
[13] J. Hafner, J. Comput. Chem. 29 (2008) 2044.
[14] A. Chakrabarti and S. R. Barman, Appl. Phys. Lett. 94 (2009) 161908.
[15] M. Pugaczowa-Michalska, J. Magn. Magn. Mater. 427 (2007) 54.
[16] V. V. Godlevsky and K. M. Rabe, Phys. Rev. B 63 (2001) 134407.
[17] M. Pugaczowa-Michalska, J. Magn. Magn. Mater. 320 (2008) 2083.